Materials in the Drive Chain – Modeling Materials for the Internet of Production

9

Ali Rajaei, Marco Becker, Yuanbin Deng, Oliver Schenk, Soheil Rooein, Patricia de Oliveira Löhrer, Niklas Reinisch, Tarik Viehmann, Mustapha Abouridouane, Mauricio Fernández, Christoph Broeckmann, Thomas Bergs, Gerhard Hirt, Gerhard Lakemeyer, and Georg J. Schmitz

Contents

A. Rajaei (✉) · Y. Deng · O. Schenk · S. Rooein · C. Broeckmann
Institute for Materials Applications in Mechanical Engineering (IWM), RWTH Aachen University, Aachen, Germany
e-mail: a.rajaei@iwm.rwth-aachen.de; y.deng@iwm.rwth-aachen.de; o.schenk@iwm.rwth-aachen.de; s.rooein@iwm.rwth-aachen.de; c.broeckmann@iwm.rwth-aachen.de

M. Becker · P. de Oliveira Löhrer · M. Abouridouane
Laboratory for Machine Tools and Production Engineering (WZL), RWTH Aachen University, Aachen, Germany
e-mail: m.becker@wzl.rwth-aachen.de; P.oliveira_loehrer@wzl.rwth-aachen.de; M.Abouridouane@wzl.rwth-aachen.de

N. Reinisch · G. Hirt
Institute of Metal Forming (IBF), RWTH Aachen University, Aachen, Germany
e-mail: niklas.reinisch@ibf.rwth-aachen.de; gerhard.hirt@ibf.rwth-aachen.de

T. Viehmann · G. Lakemeyer
Knowledge-Based Systems Group (KBSG), RWTH Aachen University, Aachen, Germany
e-mail: viehmann@kbsg.rwth-aachen.de; gerhard@informatik.rwth-aachen.de; gerhard@kbsg.rwth-aachen.de

C. Brecher et al. (eds.), *Internet of Production*, Interdisciplinary Excellence Accelerator Series, https://doi.org/10.1007/978-3-031-44497-5_23

Abstract

In this chapter, the focus lies on a predictive description of the material response to the thermomechanical loads within different process steps by means of physical and data-driven models. The modeling approaches are demonstrated in examples of innovative production technologies for components of a drive chain: Fine blanking of parts; powder metallurgical (PM) production of gears; open-die forging and machining of drive shafts. In fine blanking, material, process, and quality data are acquired to model interactions between process and material with data-driven methods. Interpretable machine learning is utilized to non-destructively characterize the initial material state, enabling an optimization of process parameters for a given material state in the long-term. The PM process chain of the gear includes sintering, pressing, surface densification, case hardening, and finishing by grinding. Several modeling and characterization approaches are applied to quantitatively describe the microstructure evolutions in terms of porosity during sintering, density profile after cold rolling, hardness and residual stresses after heat treating and grinding and the tooth root load bearing capacity. In the example of the open-die forging, a knowledge-based approach is developed to support the decision-making process regarding the choice of the proper material and optimized pass schedules. Considering the microstructure of the forged shaft, the elastoplastic material behavior is described by a dislocation-based, multiscale modeling approach. On this basis, process simulations could be carried out to predict the process forces, chip form, residual stresses, and the tool life among other output data.

9.1 Introduction

In the Cluster of Excellence "Internet of Production" at the RWTH Aachen University, a research domain is dedicated to materials. The main objective of this research domain is to provide digital tools to design dynamic production scenarios and condition-based monitoring of components, based on the knowledge about the material and components' properties. To this end, data are integrated from production and usage into physical and data-driven material models and digital material shadows are generated. This chapter contains three different process

M. Fernández · G. J. Schmitz
ACCESS e.V, Aachen, Germany
e-mail: m.fernandez@access-technology.de; G.J.Schmitz@access.rwth-aachen.de

T. Bergs
Manufacturing Technology, Laboratory for Machine Tools and Production Engineering (WZL), RWTH Aachen University, Aachen, Germany

Fraunhofer Institute for Production Technology (IPT), Aachen, Germany
e-mail: t.bergs@wzl.rwth-aachen.de

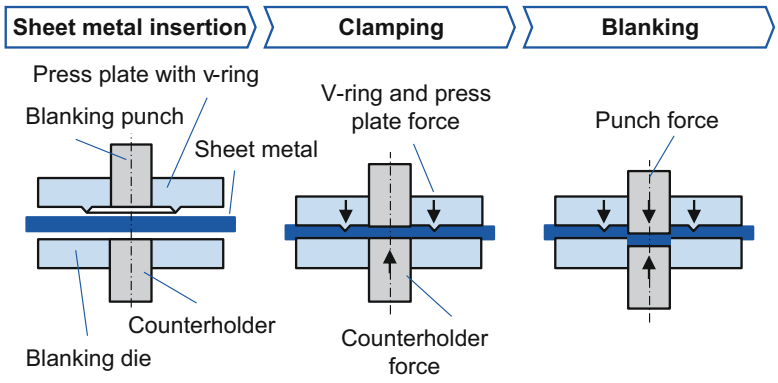

Fig. 9.1 Process steps in fine blanking

chains, chosen to demonstrate different approaches for modeling the materials in manufacturing processes within the context of the integrated computational materials engineering (ICME) and integrated structural health engineering (ISHE).

9.1.1 Fine Blanking

Fine blanking is a sheet metal shearing process. Compared to conventional blanking, fine blanking is characterized by a high geometric accuracy and a smooth shearing surface with only small tear-off (Aravind et al. 2021; Bergs et al. 2020). Fine blanking is used in mass productions of parts, e.g., for the automotive or aerospace industry (Pennekamp et al. 2019). Figure 9.1 depicts steps of the fine blanking process. First, the sheet metal is inserted into the tool. Next, the sheet metal is clamped between a press plate with a v-ring and a cutting die. Finally, the blanking takes place, before the blanked workpiece is ejected.

Despite the high precision of fine blanking, practitioners observe fluctuations in workpiece quality for fixed process parameters. These variations occur on batch level, but also along single sheet metal coils. For other sheet-metal processing manufacturing processes, research has already shown that deviations in product quality occur due to variations in material properties (Unterberg et al. 2021). A fine blanking line was equipped with sensors to capture material, process, and quality data to allow for a data-driven modeling of dependencies between material state, process state, and the resulting product quality in the long term (Niemietz et al. 2020).

9.1.2 High-Strength Sintered Gear

The powder metallurgical (PM) manufacturing of typical sintered gears usually includes powder preparation, e.g., by mixing a metal powder, pressing, and sintering

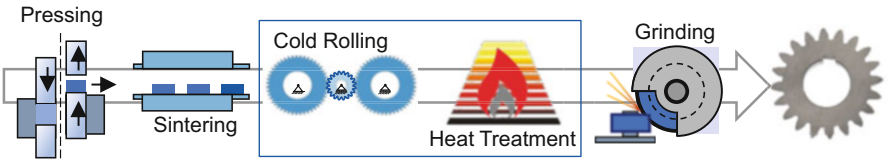

Fig. 9.2 Schematic representation of the PM process chain of high strength sintered gears

(Fig. 9.2). Some advantages of the PM route are the reduction of the material use and energy consumption in the production chain, flexibility in shape optimization, and better noise-vibration-harshness behavior of the gear (Kruzhanov and Arnhold 2012; Leupold et al. 2017). However, the strength of sintered gear is significantly lower than conventional gears, due to the remaining porosity after sintering. Further mechanical and thermal post-treatments are required, if highly loaded applications are considered for the sintered gear. Studies have shown that surface-densified and case-hardened sintered gears can achieve comparable levels of the load-bearing capacity of conventional gears (Gräser et al. 2014; Kotthoff 2003). Different modeling and simulation methods are carried out to study the process-material relation, aiming at an optimized process design for improved performance. The processes of sintering, case hardening, and grinding are highlighted in the following sections.

9.1.3 Drive Shaft

A drive shaft is a highly stressed component that is used in drive chains of various machines to transmit power and mechanical loads. In order to withstand the high, cyclical loads during their service life, the components must have excellent material properties. To this end, drive shafts, e.g., in vehicles, are often manufactured using a multi-stage production chain comprising hot forging, heat treatment, and (finish) machining (Zhao et al. 2019) (Fig. 9.3).

Despite the high level of standardization in modern manufacturing processes, hardly explainable fatigue events happen during the service life of highly loaded parts like axles or drive shafts in different machines like vehicles (Barbosa et al. 2011) or (bucket wheel) excavators (Savković et al. 2012). The reasons for these catastrophic failures, besides geometrical features, include defects regarding the local material properties like grain sizes and the surface integrity resulting from the individual manufacturing process chain (Zhao et al. 2019). To enable the tracking of the production process of individual components, a digital model of the production chain is created. Different methods including ICME-based material and process simulation approaches and knowledge-based systems are used to build a basis for developing a digital shadow that enables component-related assessments, e.g., on the unique service life (ISHE) in the long run.

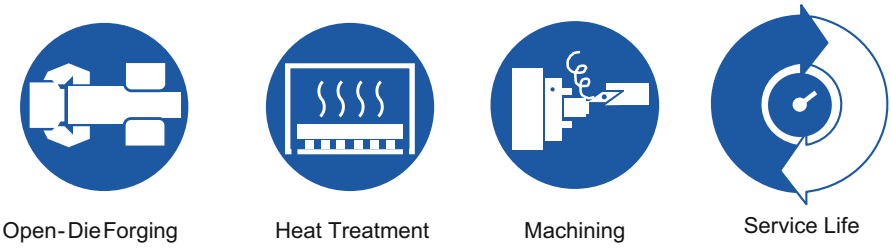

Fig. 9.3 Schematic representation of the process chain of a drive shaft

9.2 Fine Blanking – Artificial Intelligence (AI) for Sheet Metal Hardness Classification

As stated earlier, the quality of fine blanked parts varies, even without changing the process settings. Moreover, research has already shown that fluctuations in material properties lead to quality deviations in other sheet-metal processing manufacturing processes. If a digital shadow representing the actual properties of the material was available, it would provide a basis to develop an integrated model connecting material properties, process parameters, and quality parameters with the aim to adaptively control the fine blanking process based on a given material state.

One potential approach contributing to a digital material shadow is the so-called magnetic Barkhausen effect. Inside ferromagnetic materials are magnetic domains. These domains, which are separated by so-called domain walls, are regions in which the magnetic moments are aligned in one direction. When a time-dependent external magnetic field is applied to a ferromagnetic material, the domain walls move. However, the domain wall movement is hindered for example by dislocations, voids, or second-phase particles. Once the external magnetic field exceeds the restraining force of these obstacles, the domain walls break free causing jumps in the rate of magnetization of the ferromagnetic material (Jiles 2000). These Barkhausen jumps are measurable, e.g., with an inductive sensor. The resulting time series signal is called magnetic Barkhausen Noise (MBN). Due to its dependency on microstructural properties, the MBN is used for non-destructive material classification. The measurement of MBN is even fast enough to be applied in production lines (Franco et al. 2013).

Unterberg et al. (2021) conducted experiments on deep learning to classify the hardness of specimen from a 16MnCr5 (AISI: 5115) sheet-metal coil used for fine blanking based on MBN signals. They demonstrate that deep learning models, more precisely InceptionTime (Ismail Fawaz et al. 2020), allow to distinguish different classes of hardness. While deep learning is capable of learning complex relationships from raw data without manual feature engineering (Goodfellow et al. 2016), the inner complexity of artificial neural networks also renders their decision logic opaque to humans (Došilović et al. 2018). If models are only evaluated based on their prediction accuracy, it is unclear whether a model learned

plausible relationships or just exploits misleading spurious correlations (Chattopadhyay et al. 2019). Moreover, potentially unknown (and correct) relationships learned by a model remain hidden from humans, preventing humans to learn from AI. Consequently, methods to interpret or explain machine-learning models (explainable AI) are required. Establishing explainable AI in manufacturing contributes to the vision of an Internet of Production, where every production step is seen as a potentially valuable experiment from which knowledge is gained.

Several explainable AI approaches, such as Grad-CAM (Selvaraju et al. 2020), explain model predictions by highlighting parts of the input data, which are most relevant to the prediction. However, such explanations leave much room for interpretation. For instance, if a region in an MBN signal is highlighted as being important, it is still ambiguous what properties (e.g., amplitudes, frequencies, peak values, peak positions, etc.) of that region are decisive for the model prediction. Li et al. (2018) propose an alternative approach. They present a neural network architecture and an objective function enabling to learn representative examples of the classes that are to be predicted by the model. The model derives its predictions based on similarity to these representative prototypes.

Experiments with an adapted version of Li et al.'s model architecture were conducted with the aim to classify the hardness of specimen from a 16MnCr15 fine blanking steel based on MBN measurements. Figure 9.4 depicts boxplots visualizing the hardness values of the used specimen, the final accuracies of the model for training data and validation data as well as learned prototypes. The hardness and the MBN were measured at eight different spots for each specimen. MBN signals were measured over a duration of 1 s at each spot, which were divided into subsignals with a length of approx. 3.3 ms as input for the neural network. For detailed information on the data acquisition refer to Unterberg et al. (2021).

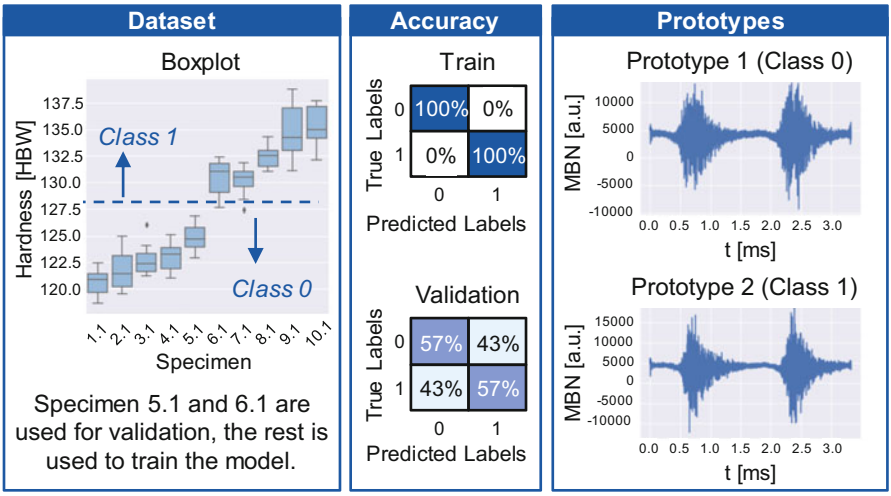

Fig. 9.4 Summary of experiments on interpretable hardness classification with deep learning

The reached validation accuracies are considerably lower than those of Unterberg et al. (2021). However, it becomes possible to compare the neural network's decision logic to existing domain knowledge, by checking whether the prototypes are consistent with findings reported in the literature on MBN. The learned prototypes appear to contradict relationships found in the literature. For instance, Franco et al. (2013) report that the peak height of the MBN decreases with increasing hardness. The prototypes suggest the opposite. Considered together with the validation accuracy, this indicates that the neural network probably did not learn the underlying relationships correctly in this case.

Balancing the optimization of the prediction accuracies and the representativeness of the learned prototypes turned out to be challenging for the given application of hardness prediction. For the approach to become valuable in practice, future work must enable higher prediction accuracies (on validation data), e.g., through an optimized architecture .

9.3 Sintered Gear – Simulation of Sintering

The compaction of water-atomized powder and its subsequent consolidation during the sintering process are decisive for the mechanical properties of a PM component. This is due to the fact that these processes can largely determine the porosity and the shape of the pores. The pore fraction and morphology have a decisive impact on the materials' fatigue strength as well as the surface densification, hardenability, grindability, and performance of the gear. Hence, a multiscale modeling approach is developed to predict the porosity and pore morphology, representing a digital material shadow in the powder compaction and sintering.

The filling of a die with Astaloy 85Mo (FE + 0.85% Mo + C) powder and its compaction can be described by a discrete element approach that aims for the modeling of the interaction between powder particles based on Newton's laws of motion. The particles are defined as agglomerates of spheres that can only undergo elastic deformation. The motion and deformation of each sphere are related to the sum of the forces F_{ij}^{sum} that act between two elements i and j:

$$F_{ij}^{sum} = F_{ij}^{Con} + F_{ij}^{Coh} + F_{i}^{Grav} \tag{9.1}$$

The contact force F_{ij}^{Con} is calculated by the Hertz-Mindlin model, while the cohesive force F_{ij}^{Coh} represents an additional normal force based on the simplified model of Johnson-Kendall-Roberts. F_{i}^{Grav} includes gravitational forces as well as the contribution of the applied pressure during compaction. Using this approach, the density distribution that is attributed to the friction between the powder and the die as well as between adjacent powder particles can be assessed (Luding 2008).

Static properties, such as the tensile strength, are mainly related to the density distribution, whereas the estimation of the fatigue behavior requires a more detailed assessment of the microstructure. This can be achieved by the application of machine learning. In the field of image generation, generative adversarial networks (GAN) have been applied to a vast variety of problems. A GAN consists of two neural networks, which are referred to as Generator and Discriminator. The former converts an input vector of random values into an image, while the latter is trained to distinguish between generated images and the training dataset. The response of the Discriminator is used to optimize both neural networks. If the training process is evenly balanced, the Generator is empowered to create images that are sufficiently accurate. To account for the influence of relevant variables such as process parameters, an underlying taxonomy is required. Numerical labels are assigned to the images that translate the related process or data conditions, including information such as powder particle size and the magnification of the used microscope. These labels are then embedded in the training process. Linear interpolation techniques, applied to a trained model, enable the prediction of images for new process conditions (Azuri and Weinshall 2020; Goodfellow et al. 2016).

The sintering process is driven by the local gradient of the chemical potential that is directly related to the local curvature. Depending on the temperature, different diffusion mechanisms contribute to the formation of sintering necks and the rounding of pores. Higher sintering temperatures induce a significant contribution of grain boundary and volume diffusion, provoking commonly undesired shrinkage (German 1996). Hence, sintering of conventional PM steel is normally carried out at 1120 °C to mainly activate surface diffusivity, which ensures dimensional stability. Therefore, a mesoscale model primarily requires a physical description of surface diffusion only. The local velocity of the surface of a pore can be described by the surface mobility M and the divergence of the local curvature κ:

$$v = M \cdot \Delta_S \kappa \tag{9.2}$$

The mobility includes the contributions of the surface diffusion coefficient D_S, the surface layer thickness δ, the atomic volume Ω, and the surface energy γ:

$$M = \frac{D_S \delta \gamma \Omega}{kT} \tag{9.3}$$

with T as the temperature and k as the Boltzmann constant.

Instead of modeling the geometry of the powder particles, a level-set-function ϕ is used to continuously describe the interface of the powder and the pore as a signed distance function. The divergence of this function provides the curvature at the surface of the particles. The evolution of the curvature as a function of the time t can be simulated by explicitly solving the advection equation (Bruchon et al. 2012):

$$\frac{\partial \phi}{\partial t} + v \nabla \phi = 0 \tag{9.4}$$

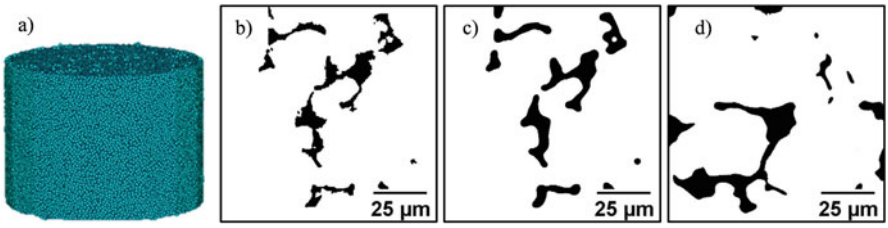

Fig. 9.5 Simulation result of powder die compaction (**a**), predicted microstructure after compaction (**b**), simulated evolution of the microstructure during sintering (**c**), and the corresponding microstructure observed in experiments (**d**)

The methods were merged to predict the microstructure after sintering based on process parameters of compaction and sintering. The GAN was trained for 500 epochs with binary images taken from green samples with variable particle sizes, which were included as image labels. For image recording in the scanning electron microscope, the samples were first embedded and infiltrated with cold resin, then ground and polished following the standard metallographic procedure. After the training, spherical linear interpolation was applied to generate images for a particle size range between 32 and 128 µm.

The feasibility of the proposed method is demonstrated by comparing the results of the model with microstructural images from experiments. Figure 9.5a depicts the simulation results of the compaction process on the macroscale, while Fig. 9.5b shows an image with a size of 100 × 100 μm^2 that represents the predicted microstructure with a mean particle size of 83 µm. The subsequent sintering process was assumed to be isothermal at a temperature of 1120 °C with a holding time of 48 min. The simulation result is presented in Fig. 9.5c. The corresponding experimental result, conducted in a quenching dilatometer under vacuum, is displayed in Fig. 9.5d. The predicted pore morphology conveys a good agreement with the experiment.

9.4 Sintered Gear – Surface Hardening and Load-Bearing Capacity

The local surface densification of sintered gears is a promising technique to increase the load bearing capacity drastically. Common methods to densify the functional surfaces of sintered gears are shot peening and cold rolling (Frech et al. 2017). To further increase the material's strength and thus the load-bearing capacity of the gear, a case hardening treatment is conducted after the surface densification. Basically, same processes can be applied to heat-treat sintered parts as in the case of wrought steel parts. However, the effect of the porosity on the material response and the final result of the heat treatment should be considered to choose the optimal

treatment strategy and process parameters (Danninger and Dlapka 2018). To study the potential in optimizing the bearing capacity by surface densification and case hardening, an ICME approach is developed, which links simulation blocks that consecutively represent the process steps of carburizing, quenching, tempering and loading of the gear.

Prior to the actual modeling, the density profile in the cross section of the tooth is determined by image analysis of the microstructure and then mapped to the model geometry. The micrographs are transformed into binary images, in which material is represented by white and pores by black pixels. The density of a given area is obtained from the ratio of black and white pixels (Fig. 9.6a). The macro-scale heat treatment model applied in the present work is a finite element modeling approach that comprises the calculation of diffusion, heat transfer, phase transformations, transformation strains, and the elastoplastic material response. Carbon diffusion during carburizing is calculated by the Fick's laws, enabled by defining the temperature-dependent diffusion coefficient and setting corresponding boundary conditions. To model the quenching and tempering stages, a coupled thermomechanical analysis is carried out. The main constitutive law in the mechanical

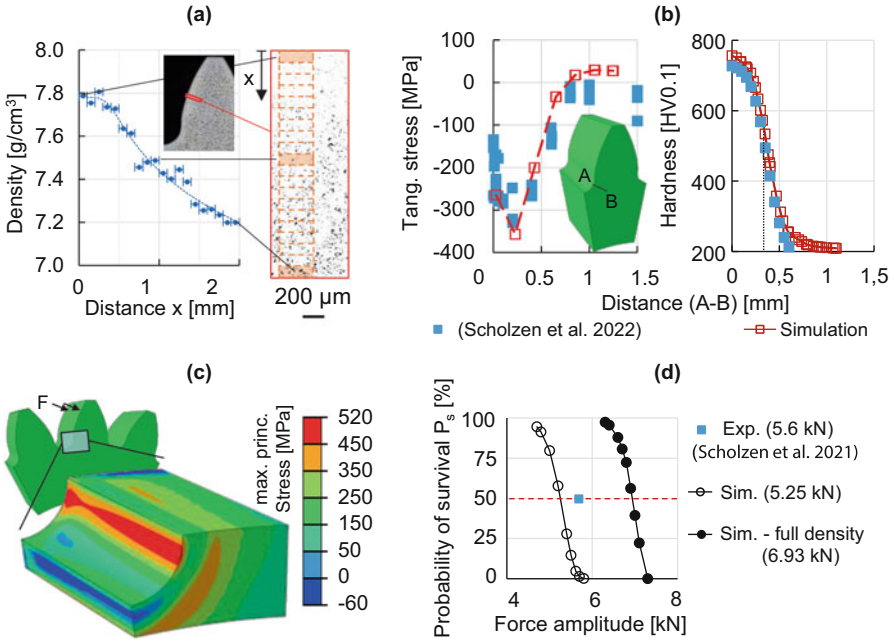

Fig. 9.6 Graphical overview of the modeling approach to predict the load-bearing capacity of a surface-hardened sintered gear, with a module of 3.175 mm and a case hardening depth of 0.3 mm. (**a**) Determination of the density profile, (**b**) simulation of the case hardening, (**c**) simulation of the tooth root bending, and (**d**) calculated load bearing capacity of the tooth root

analysis describes the evolution of the strain tensor and assumes that the total strain rate equals the sum of independent elastic, plastic, thermal, and transformation induced strain rates. The microstructure is described as a continuum, containing calculated volume fractions of different microstructural phases. To describe the overall kinetics of the phase transformations, modified formulations and extensions of the Koistinen-Marburger equation (Koistinen 1959) and the Johnson-Mehl-Avrami-Kolmogorov (JMAK) equation (Avrami 1941) are applied for the martensitic and the diffusion-controlled transformations, respectively. Thermophysical properties of the material are defined depending on the temperature, density, phase fractions, and carbon content. The simulated residual stress state is transferred as the initial stress tensor to the simulation of the loading. Hence, the residual stress is automatically superimposed to the stress tensor resulting from the external loading. More details about the modeling approach are found in Rajaei et al. (2021). Figure 9.6b, c show the simulated hardness and residual stress profiles after case hardening as well as the stress state under loading with a F = 5.25 kN force.

The calculation of the load-bearing capacity is carried out in a post-processing analysis. For each integration point of the FE-model, the local stress and strength values are compared in terms of the local degree of utilization A(x, y, z), i.e., the ratio of the applied equivalent stress amplitude to the fatigue strength under uniaxial loading. The equivalent stress amplitude is determined for a given time-dependent stress tensor according to a proper fatigue criterion, which considers the mean stress effect and multiaxiality. For the example of the tooth root bending, the simple normal stress criterion is still valid, due to the nearly proportional loading case, i.e., constant principal stress directions (Brömsen 2005). The local fatigue strength is calculated for the sintered steel Astaloy Mo85 according to the model suggested in Hajeck et al. (2018), which is developed based on bending fatigue experiments on laboratory samples. The model defines the fatigue strength depending on the density, highly loaded volume, and carbon content, which can be reformulated in terms of hardness. Having the local degree of the utilization, the probability of survival P_s can be obtained as follows:

$$P_s = 2^{-\frac{1}{V_0}\int A(x,y,z)^{k(x,y,z)}dV} = 2^{-\frac{1}{V_0}\sum\left(A_i{}^{k_i}\right)\cdot V_i} \tag{9.5}$$

where V_0 is a reference volume equal to 1 mm^3, k_i is the Weibull module of the integration point i in the FE-model, which accounts for the statistical size effect, and V_i is the volume of the integration point i. The load-bearing capacity is the external force for a survival probability of 50%. Figure 9.6d summarizes the calculation of the tooth root load-bearing capacity. The predicted residual stress and hardness profiles agree very well with experimental results from Scholzen et al. (2022). In Fig. 9.6d the expected bearing capacity of the gear without porosity is given, 6.93 kN. According to the simulation, porosity reduces the bearing tooth root capacity by approximately 25%, compared to a gear with full density.

The prediction of the tooth flank bearing capacity requires a more sophisticated fatigue criterion that is valid for a non-proportional loading and is an ongoing work.

9.5 Sintered Gear – Grinding and Surface Integrity

Grinding is a widely used hard finishing process in gear manufacturing due to high dimension accuracy and improvement of the surface integrity. Currently, the definition of suitable process parameters is performed by elaborate trials or based on the operator's experience. Alternatively, several models for description of grinding loads have been developed for the process of gear grinding in order to regulate the process and to define suitable parameters. However, these models are in general time consuming, which limits their application in production line. In addition, process monitoring for the regulation of the process can also be a challenging task in gear grinding processes due to complex process characteristics. The main objective of this project section is the optimization of the procedure for generating gear grinding with a focus on surface integrity by means of a networked adaptive production concept. In order to achieve this objective, the project is divided into different steps. In the first step, a new process modeling based on the digital twin concept will predict the energy generation according to the material removal rate, given by process parameters and kinematics. In the second step, solutions for real-time measurement methods will be investigated, as well as a connection between real-time measurements and the energy model outputs. Finally, in order to support a wider application of the optimized grinding procedure, a data lake will be built to store relevant data regarding the process under different conditions.

In the following, an explanation of the current status of the first step of the project, regarding the new process modeling is explained. During grinding, a major percentage of the generated energy is converted into heat. Most fraction of this heat is transferred into the gear, and may cause thermal damages. In order to better understand and control the part of the generated heat that flows into the gear, it is first necessary to specify the according energy partition. In the work of Hahn (1966), it was established that the material is removed by each grain of the grinding tool along three different mechanisms: friction, plowing, and shearing. Each of these mechanisms contributes in a singular way to the partition of energy that goes into the gear (Linke et al. 2017). The energy generated in each of the three mechanisms depends on grain-gear micro-interaction characteristics (Malkin and Guo 2007). These micro-interaction characteristics are influenced by the grinding tool topography. The interaction between the grains and the gear is characterized based on both process kinematics and parameters. In order to develop a suitable grinding energy calculation for the generating gear grinding, it is necessary to first consider the single-grain interaction in the contact zone, based on the process parameters.

For the process model developed in this project section, an existing simulation model of the generating gear grinding process based on penetration calculation approach is used. An extension of this simulation model considering a realistic modeling of the topography and the rotational movement of the grinding worm during the process is performed. As a result of the simulation, micro-interaction characteristics for each of the engaging grains are obtained and used for the calculation of the energy in generating gear grinding.

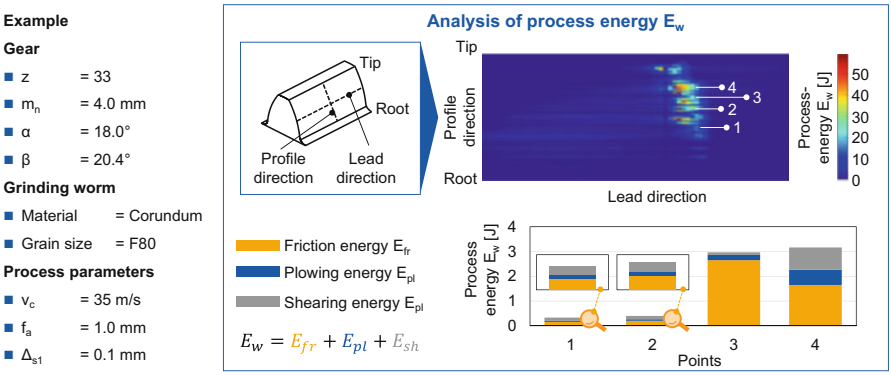

Fig. 9.7 Analysis of the energy calculation for generating gear grinding process

The results of the process energy E_w calculated with the extended simulation model are shown in the upper right of Fig. 9.7. The gear, grinding worm, and process parameters used for the calculation are shown in the left side of Fig. 9.7. For better visualization, the calculated process energy E_w was plotted onto the flank of the gear. In the visualization, the process energy E_w corresponds to the energy generated by grinding in one specific axial position. Therefore, only one area of the gear flank was ground in the simulation, and not the entire flank.

In the four points highlighted in Fig. 9.7, a further analysis of the energy was performed, which is shown in the diagram in the lower right side of Fig. 9.7. For the points one and two, similar process energies and contributions are obtained. In the points three and four, the process energies E_w are also similar to each other, but the contributions of each individual energy of each chip formation mechanism are different. The importance of an analysis of the process energy E_w considering the chip formation mechanisms is due to the fact that each of these mechanisms has a different partition of energy that goes into the gear. According to Malkin (Linke et al. 2017), almost all the friction energy E_{fr} is conducted as heat to the gear, while for plowing E_{pl} and shearing E_{sh} energies, this fraction is smaller. The fraction of energy conducted as heat to the gear for the shearing mechanism is the lowest of the three mechanisms (Linke et al. 2017). Therefore, if a significant part of the process energy E_w corresponds to shearing energy E_{sh}, most of this energy is used for chip removal and not to heat to the gear. If most of the process energy is not converted to heat, the possibility of grinding burn during the process decreases. Due to this, even though the points three and four presented similar process energies E_w, the contribution of each individual energy of each chip formation mechanism is different for each of these points, leading to different amounts of heat transferred into the gear. Based on these results, the method for the calculation of the process energy E_w for generating gear grinding was able to show sensible outcome. Ultimately, this method can be used in the future for the prediction of grinding burn for the generating gear grinding. For this, the critical values of the individual energy of each chip formation mechanism and their influence on the grinding burn presence need to be defined.

9.6 Drive Shaft – Open-Die Forging

Open-die forging is a bulk metal forming process that can be used to produce mostly longitudinally oriented components such as drive shafts or axles with excellent material properties. In open-die forging, the ingot is incrementally formed into the desired shape using two simple dies that perform so-called strokes. Forging processes are summarized in pass schedules that contain the important process parameters like height reductions or press velocities for each individual pass. A forging pass consists of a discrete number of consecutive strokes that are oriented in the same ingot direction and hence, deform a defined region of the ingot.

Since commonly hundreds of individual strokes can be involved in an open-die forging process, there are a large number of process routes that lead to the same final geometry. However, these different processes are not equivalent from a production point of view, as they have different process times, energy consumption and, most importantly, can produce different material properties in the final part. Therefore, both the targeted process design and the detailed monitoring and tracking (digital shadow) of individual open-die forging processes as well as their corresponding down- and upstream processes are very useful for the reliable and efficient production of forgings with excellent material properties.

Since important material and workpiece properties often cannot be measured directly during the open-die forging process, an assistance system for open-die forging was developed that is able to monitor the current state of the forging ingot live, throughout the process (Rudolph et al. 2021). Besides information on temperature and geometry, the equivalent strain introduced along the core fiber is determined using a fast calculation model. Afterward, the combined time-dependent information on temperature and equivalent strain enables the calculation of the grain size present insight of the ingot during and after forging, using a fast material model based on JMAK-equations (Karhausen and Kopp 1992) (ICME) and hence, laying the foundation for a digital shadow of the forged component. The process data insight of the digital shadow can be used to subsequently set up an FE-model and hence, to enrich, e.g., locally restricted information from the fast process models. Here, for example, three-dimensionally resolved temperature and equivalent strain trajectories can be generated and incorporated back into the fast microstructure model to calculate a three-dimensional distribution of the grain size in the component over the course of the forging.

Although the process route has a decisive influence on the component quality, the process design in open-die forging is still often based on experience or simple models, resulting in a need for new approaches on the targeted process design. Since compared to, e.g., die casting, which is used for producing high-volume batches, the batch sizes in open-die forging are rather small. Hence, data from real forgings is not widely available, limiting the usability of modern data-driven algorithms that require large amounts of data for their application. Therefore, a case-based reasoning (CBR) (Richter and Weber 2016) agent for the targeted design of pass schedules for the open-die forging process is developed. Similar to the human

experience-based behavior, CBR is a methodology to learn based on experience by remembering past problems (cases) and the way they were solved (solutions). By recording data of past forging processes (digital shadows) and complementing those with data of simulations and fast process models, the CBR-agent shall make suitable recommendations for a new case that requires a pass schedule. However, it is not sufficient to consider individual steps in a production chain of products. Decisions to be made range from the material selection, heat treatment specifications, press and tool allocation, and pass schedule layout to the final machining steps. Typically, the required knowledge to make informed decisions is spread across different stakeholders (cf. Fig. 9.8). For example, the material choice for a drive shaft, considering a set of requirements, may depend not only on the prices and availability of the different steel alloys at the retailer ("steel retailer"), but also on the available material characteristics required to simulate and design the forging process ("IBF-agent") as well as the heat treatment strategy ("IWM-agent") or the machining process ("WZL-agent").

While the internet is heavily used in the everyday lives to accumulate information, there is typically no unified network between different industrial stakeholder, which could be used for planning complex manufacturing processes. A decentralized World-Wide-Lab (WWL) infrastructure, where companies and research labs can offer their services, is required in order to solve such complex tasks efficiently, supported by autonomous agents. A service agent may range from simple data vendors, e.g., a retailer (cf. Fig. 9.8, "steel retailer") informing about prices and availability, to complex process control nodes that automatically interact with other's agents in the WWL, in order to accumulate data to plan out the manufacturing process for a whole product. The WWL ensures semantic interoperability between the different agents through the use of ontologies. Interfaces are specified using the Thing Description ontology (Kaebisch et al. 2020) and agents need to agree on a core ontology that structures the information about production processes. Individual agents may extend this core ontology, if needed.

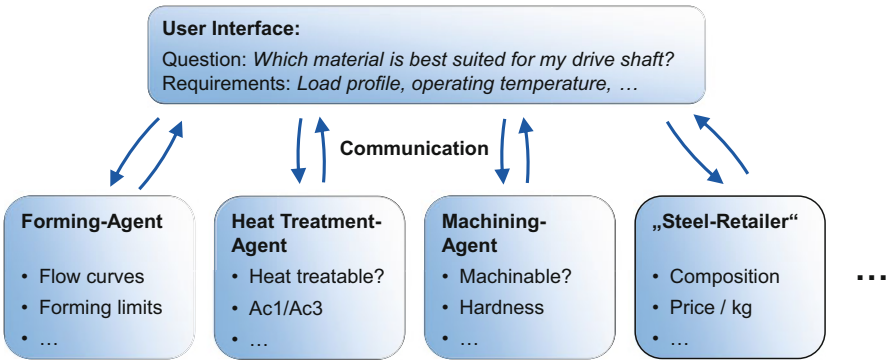

Fig. 9.8 Schematic representation of communicating WWL-agents of different process steps for solving an exemplary production-related problem

Data provenance information plays an integral role in the vison of a WWL, hence several requirements specified in the FactDAG model (Gleim et al. 2020) for data provenance information are covered by WWL agents. Agents need to be able to find other participants of the WWL, so that they are aware of possible collaboration opportunities. To keep the structure decentralized, each agent maintains a local service cache that can be expanded by scanning the network via User Datagram Protocol (UDP) multicasts.

Combining the digital shadow, e.g., of each forged drive shaft with the new possibilities of the WWL it shall be possible to adapt subsequent manufacturing steps such as heat treatment or mechanical processing based on the previous individual manufacturing process. Moreover, assumed the digital shadow of a forged drive shaft is complemented by component-specific information on the downstream production processes, an individual long-term estimate of, e.g., the service life of the component (ISHE) might be possible in the long run.

9.7 Drive Shaft – Machinability

The machinability of a material is one of the most important input parameters for an optimized process design. It determines, apart from the tool wear and the achievable chip removal rates, the surface integrity as well as the functionality of the finished component. The machinability of a material is dependent on the microstructure, controlled by the chemical composition and the heat treatment state, and thus offers a very wide field in the area of basic research and industrial application (Abouridouane et al. 2019).

In order to determine the influence of the microstructure on the machinability of drive shaft, a new experimental setup with automatic multi-sensor data acquisition has been developed for in-process measurement of thermo-mechanical load and tool wear during turning operations (see Fig. 9.9). In order to check the performance of the proposed experimental setup and to derive correlations between the operating thermo-mechanical load and the machined surface characteristics, longitudinal finish turning tests on drive shafts made of steel 42CrMo4 with two different microstructures are carried out using carbide indexable inserts.

A summary of the main results obtained in the present research work can be given as follows:

- The proposed experimental setup is suitable for in-process measurement and analysis of the thermo-mechanical load and tool wear by turning operations.
- The thermo-mechanical load, which depends to a large extent on the hardness of work material, controls the tool wear and the resulting surface finish as well as the induced residual stresses.
- The measured roughness R_z shows obviously the bad influence of the tool wear on the achieved surface quality when finish turning drive shaft.
- The achieved surface integrity results can be incorporated in digital twins for process monitoring to optimize cutting process performance.

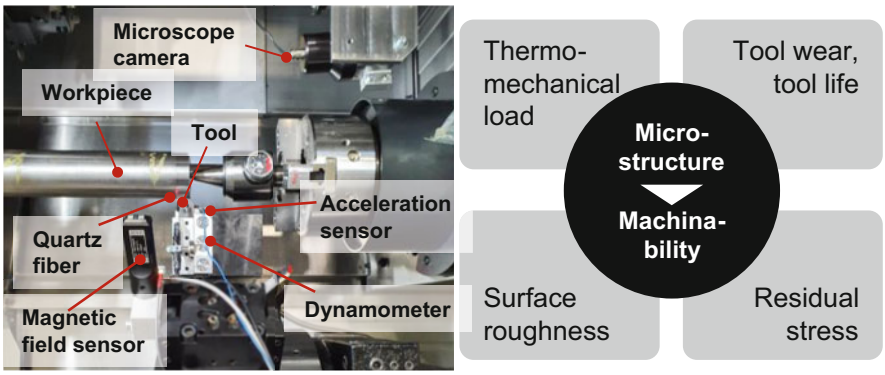

Target quantity (mean values)	Shaft 1	Shaft 2
Hardness / HRC	26	24.8
Cutting force / N	120	110
Surface temperature / °C	85	70
Tool flank wear VB / µm	115	98
Surface roughness R_z / µm	6.6	4.6
Residual stress / MPa	390	210

Workmaterial:	42CrMo4	Cutting speed:	150 m/min
Tool:	CNMG 120408-PM 4315	Feed:	0.15 mm
Cooling:	Dry cut	Depth of cut:	0.5 mm

Fig. 9.9 Multi-sensor experimental setup for machinability characterization

A multiscale approach was developed to predict the mechanical yielding behavior of the work material and thus its machinability. The modeling of the constitutive behavior of the considered materials poses several challenges at different levels. All following assumptions and models follow closely the choices of Laschet et al. (2022).

First, the elastic and plastic behavior of pearlite and ferrite must be modeled. For ferrite, a cubic elastic behavior is considered and its plastic behavior is assumed to be governed by a dislocation-based approach, which then determines the corresponding yield stress. Here, the dislocation density ρ is assumed to be governed in terms of the plastic strain ϵ_p by the following approach (modified Kocks-Mecking-Estring model) (see Laschet et al. 2022 for details).

$$\frac{d\rho}{d\epsilon_p} = M\left(\frac{k_1}{b}\left(1-\exp\left(-\psi\sqrt{\rho}\right)\right) - k_2\rho + \frac{k_3}{b\,D}\exp\left(-\frac{M\lambda^*}{b}\epsilon_p\right)\right) \tag{9.6}$$

The evolution of the dislocation density of ferrite is influenced by the parameters $p_F = (\psi, k_1, k_2)$, while all other quantities are kept constant. For cementite, its elastic behavior is assumed as orthotropic. The evolution of the dislocation density of cementite is assumed to be governed by the following approach (hardening law of Gutierrez-Altuna type):

$$\rho = \frac{1 - \exp\left(-k_2 M \epsilon_p\right)}{b k_2 L} + \rho_0 \exp\left(-k_2 M \epsilon_p\right) \tag{9.7}$$

The dislocation density of cementite and its corresponding yield behavior are assumed constant (see Laschet et al. 2022 for details).

Then, a representative volume element (RVE) is generated at the "nano" and "micro" levels. At the nano level, a bilamellar RVE representing the ferrite-cementite-structure of pearlite is generated with ABAQUS. The nano RVE considers the statistics measured in experiments, i.e., the volume fractions of ferrite and cementite and the lamellar lengths. At the micro level, a polycrystalline RVE is generated with DREAM3D, considering the microstructure statistics, e.g., average grain size, volume fractions of ferrite and pearlite.

The final yield stress curve (computed then with the nano/micro RVEs and the software HOMAT) depends then on the specific choice of the parameters for ferrite. It is further assumed that the plastic behavior of ferrite in pearlite at the nano level and in the polycrystalline arrangement at the micro level differ, such that corresponding parameters $p_{F,nano}$ and $p_{F,micro}$ (in total six parameters) are optimized separately. An optimization loop is setup in Python with the LIPO package for derivate and parameter-free global optimization built upon the C++ dlib package. In this loop, for every new set of values for the optimization variables $p_{F,nano}$ and $p_{F,micro}$, the effective elastoplastic behavior of the nano RVE is computed and passed on as the pearlite phase to the micro RVE. Then, the effective plastic behavior of the micro RVE is computed and the resulting yield behavior is compared to experimental data. The loop continues improving the parameters until a maximum number of iterations is reached. The final optimized yielding behavior at the micro level can then be passed on for macroscopic simulations.

9.8 Summary

This chapter illustrated several approaches to model materials' response along a wide range of manufacturing processes. In general, the common objective is a predictive and quantitative description of the process-microstructure-property interactions on different time and length scales. However, the concrete questions, target values, boundary conditions, and approaches must be defined specifically for the considered application. The presented ICME-approaches provide valuable predictions of the microstructure and accordingly the component properties by means of sophisticated physical and empirical models, i.e., digital twins, as in

the simulations of the sintering, heat treatment, and grinding. Data-driven and fast approaches, i.e., digital shadows, as in fine blanking, open-die forging and machining can be integrated into the process control and act as in-situ digital sensors that provide essential information about hard to acquire parameters. Finally, knowledge-based approaches, e.g., case-based reasoning, can link different sectors of expertise together and provide the infrastructure to integrate the material-experts' knowledge along the entire development, production, and operation cycles.

The vision of the future work is to provide robust digital tool boxes to be integrated already in the early phases of the planning and designing toward an agile product development and production. To facilitate the use of the future tool box, standard data formats should be defined for all input and output data of the models. Furthermore, codes and models should be parametrized and proper simulation platforms, e.g., AixVipMap, should be adopted to automatically run multi-step simulations and produce large data. With the help of capable database and ontology solutions, the simulation data and the knowledge gained would be collected to form a data lake. On this basis, AI methods become applicable to deepen the understanding of complex physical interactions between process, material, and components performance and give suggestions for holistic optimization of the production.

Acknowledgments Funded by the Deutsche Forschungsgemeinschaft (DFG, German Research Foundation) under Germany's Excellence Strategy – EXC-2023 Internet of Production – 390621612.

References

Abouridouane M, Laschet G, Kripak V, Dierdorf J, Prahl U, Wirtz G, Bergs T (2019) Microstructure-based approach to predict the machinability of the ferritic-pearlitic steel C60 by cutting operations. Procedia CIRP 82:107–112. https://doi.org/10.1016/j.procir.2019.04.013

Aravind U, Chakkingal U, Venugopal P (2021) A review of fine blanking: influence of die design and process parameters on edge quality. J Mater Eng Perform 30:1–32

Avrami M (1941) Granulation, phase change, and microstructure kinetics of phase change. III. J Chem Phys 9:177–184

Azuri I, Weinshall D (2020) Generative latent implicit conditional optimization when learning from small sample. In: 25th International Conference on Pattern Recognition (ICPR). IEEE, Milan, pp 8584–8591

Barbosa C, Do Nascimento JL, Caminha IMV, de Cerqueira Abud I, de Carvalho SS (2011) A microstructural and fractographic study on the failure of a drive shaft. J Fail Anal Prev 11:693–699

Bergs T, Niemietz P, Kaufman T, Trauth D (2020) Punch-to-punch variations in stamping processes. In: 2020 IEEE 18th World Symposium on Applied Machine Intelligence and Informatics (SAMI). IEEE, Milan, pp 213–218

Brömsen O (2005) Steigerung der Zahnfußtragfähigkeit von einsatzgehärteten Stirnrädern durch rechnerische Zahnfußoptimierung. Dissertation, RWTH Aachen University

Bruchon J, Pino-Muñoz D, Valdivieso F, Drapier S (2012) Finite element simulation of mass transport during sintering of a granular packing. Part I. Surface and lattice diffusions. J Am Ceram Soc 95:2398–2405

Chattopadhyay A, Manupriya P, Sarkar A, Balasubramanian VN (2019) Neural network attributions: a causal perspective. In: 36th international conference on machine learning. PMLR, Eureka, pp 981–990

Danninger H, Dlapka M (2018) Heat treatment of sintered steels – what is different? J Heat Treat Mater 73:117–130

Došilović FK, Brčić M, Hlupić N (2018) Explainable artificial intelligence: a survey. In: 2018 41st international convention on information and communication technology, electronics and microelectronics (MIPRO). IEEE, Milan, pp 210–215

Franco FA, González MF, de Campos MF, Padovese LR (2013) Relation between magnetic Barkhausen noise and hardness for Jominy quench tests in SAE 4140 and 6150 steels. J Nondestruct Eval 32:93–103

Frech T, Scholzen P, Löpenhaus C, Klocke F (2017) Influence of different manufacturing processes on properties of surface-densified PM gears. Gear Technol 35:66–77

German RM (1996) Sintering theory and practice. Wiley, New York

Gleim L, Pennekamp J, Liebenberg M, Buchsbaum M, Niemietz P, Knape S, Epple A, Storms S, Trauth D, Bergs T (2020) FactDAG: formalizing data interoperability in an internet of production. IEEE Internet Things J 7:3243–3253

Goodfellow I, Bengio Y, Courville A (2016) Deep learning. MIT Press, London

Gräser E, Hajeck M, Bezold A, Broeckmann C, Brumm M, Klocke F (2014) Optimized density profiles for powder metallurgical gears. Prod Eng 8:461–468

Hahn RS (1966) On the mechanics of the grinding process under plunge cut conditions. J Eng Ind 88:72–80

Hajeck M, Frech T, Beiss P, Broeckmann C, Klocke F, Löpenhaus C (2018) Tooth root load bearing capacity of surface densified Fe-0.85 wt.% Mo powder metallurgical gears. Int J Powder Metall 54:33–46

Ismail Fawaz H, Lucas B, Forestier G, Pelletier C, Schmidt DF, Weber J, Webb GI, Idoumghar L, Muller P-A, Petitjean F (2020) Inceptiontime: finding alexnet for time series classification. Data Min Knowl Disc 34:1936–1962

Jiles DC (2000) Dynamics of domain magnetization and the Barkhausen effect. Czechoslov J Phys 50:893–924

Kaebisch S, Kamiya T, McCool M, Charpenay V, Kovatsch M (2020) Sebastian Kaebisch, Takuki Kamiya, Michael McCool, Victor Charpenay, Matthias Kovatsch. https://www.w3.org/TR/wot-thing-description/

Karhausen K, Kopp R (1992) Model for integrated process and microstructure simulation in hot forming. Steel Res 63:247–256

Koistinen DP (1959) A general equation prescribing the extent of the austenite-martensite transformation in pure iron-carbon alloys and plain carbon steels. Acta Metall 7:59–60

Kotthoff G (2003) Neue Verfahren zur Tragfähigkeitssteigerung von gesinterten Zahnrädern. Dissertation, RWTH Aachen University

Kruzhanov V, Arnhold V (2012) Energy consumption in powder metallurgical manufacturing. Powder Metall 55:14–21

Laschet G, Abouridouane M, Fernández M, Budnitzki M, Bergs T (2022) Microstructure impact on the machining of two gear steels. Part 1: derivation of effective flow curves. Mater Sci Eng A 845:143125

Leupold B, Janzen V, Kotthoff G, Eichholz D (2017) Validation approach of PM gears for eDrive applications. In: International conference on gears, pp 119–131

Li C, Liu H, Chen C, Rudin C (2018) Deep learning for case-based reasoning through prototypes: a neural network that explains its predictions. In: Proceedings of the AAAI Conference on Artificial Intelligence, vol 32, pp 3530–3537. https://dl.acm.org/doi/abs/10.5555/3504035.3504467

Linke BS, Garretson I, Torner F, Seewig J (2017) Grinding energy modeling based on friction, plowing, and shearing. J Manuf Sci Eng 139:239

Luding S (2008) Introduction to discrete element methods: basic of contact force models and how to perform the micro–macro transition to continuum theory. Eur J Environ Civ Eng 12:785–826

Malkin S, Guo C (2007) Thermal analysis of grinding. CIRP Ann 56:760–782
Niemietz P, Pennekamp J, Kunze I, Trauth D, Wehrle K, Bergs T (2020) Stamping process modelling in an Internet of Production. Procedia Manuf 49:61–68
Pennekamp J, Henze M, Schmidt S, Niemietz P, Fey M, Trauth D, Bergs T, Brecher C, Wehrle K (2019) Dataflow challenges in an internet of production: a security & privacy perspective. In: Proceedings of the 5th ACM workshop on cyber-physical systems security & privacy. Association for Computing Machinery, New York, pp 27–38
Rajaei A, Deng Y, Schenk O, Rooein S, Bezold A, Broeckmann C (2021) Numerical modelling of the powder metallurgical manufacturing chain of high strength sintered gears. Chin J Mech Eng 34:1–18
Richter MM, Weber RO (2016) Case-based reasoning. Springer, Heidelberg
Rudolph F, Wolfgarten M, Keray V, Hirt G (2021) Optimization of open-die forging using fast models for strain, temperature, and grain size in the context of an assistance system. In: Forming the future: proceedings of the 13th international conference on the technology of plasticity. Springer, New York, pp 1145–1159
Savković M, Gašić M, Petrović D, Zdravković N, Pljakić R (2012) Analysis of the drive shaft fracture of the bucket wheel excavator. Eng Fail Anal 20:105–117
Scholzen P, Rajaei A, Brimmers J, Hallstedt B, Bergs T, Broeckmann C (2022) Influence of heat treatment and densification on the load capacity of sintered gears. In: Powder metallurgy, pp 1–8. https://doi.org/10.1080/00325899.2022.2138171
Selvaraju RR, Cogswell M, Das A, Vedantam R, Parikh D, Batra D (2020) Grad-CAM: visual explanations from deep networks via gradient-based localization. Int J Comput Vis 128: 336–359
Unterberg M, Stanke J, Trauth D, Bergs T (2021) A time series classification approach to non-destructive hardness testing using magnetic Barkhausen noise emission. Prod Eng 15:509–517
Zhao L-H, Xing Q-K, Wang J-Y, Li S-L, Zheng S-L (2019) Failure and root cause analysis of vehicle drive shaft. Eng Fail Anal 99:225–234